Mathematics Notes

Note 27

December 1972

Numerical Techniques Useful in the Singularity Expansion Method as Applied to Electromagnetic Interaction Problems.

by

T. T. Crow, B. D. Graves, C. D. Taylor
Mississippi State University
Mississippi State, Mississippi 39762

Abstract

A system of Pocklington-type integro-differential equations representing crossed cylinders has been studied by means of the singularity expansion method. The numerical techniques used to determine the natural frequencies and associated mode and coupling vectors are discussed. These results are used to determine the time domain response of the currents on the structures considered and compared to results obtained earlier by more conventional frequency analysis and Fourier inversion.

Acknowledgements

We would like to thank the following persons for valuable discussions concerning the SEM; Dr. Carl Baum, Dr. Fred Tesche, Dr. Don Wilton, and Dr. Tom Shumpert.

1. Introduction

Recently Baum [1] has discussed the singularity expansion method and its applicability to general scattering problems. Using these techniques, one can determine the natural or resonant frequencies of a particular structure and the current distributions associated with these resonances. The time domain response of the structure is then obtained as a summation of exponentially damped sinusoids, the magnitude of each being determined in a straight-forward manner.

A Pocklington type E-field integro-differential equation formulation for the induced currents on the scatterer is cast into matrix form by means of the method of moments. (A comparison of the various formulations and current expansions is made in order to estimate the rate of convergence of the particular form used.) From the resulting matrix equation, the poles or natural frequencies are found by a numerical search routine. The modes associated with each frequency are determined by standard matrix operations, and the amplitude of each damped sinusoid is determined using the derivative of the system matrix with respect to the complex frequency.

The greatest advantage of the singularity expansion technique is that one can separate and characterize basic attributes of the structure only once, and the time domain response for various types of excitation can be easily determined from the structure's characteristic behavior.

2. Formulation

The geometries considered in this study are shown in Figure 1. Tesche [2] has studied the isolated cylinder using the SEM (singularity expansion method) while others [3,4] have determined time domain responses of the cylinder in the more conventional manner - namely solving the frequency domain problem and then performing a Fourier inversion into the time domain. Also using the latter method, Taylor and Crow [4] have previously studied the crossed cylinder problem.

The starting point for this study is the Pocklington type integro-differential equation for an N-wire system [5]. For a complex frequency, $s = \sigma + jw$

$$- s \varepsilon_o 4\pi E^i(Sn) = \sum_{m=1}^{N} \int_{L_m} I_m(S'_m) \left[\frac{- \partial^2}{\partial S_n \partial S'_m} - \frac{s^2}{c^2} (\hat{S}'_m \cdot \hat{S}_n) \right] G(S_n, S'_m) dS'_m \qquad (1)$$

The thin wire approximation is used, and the kernel G has the form

$$G = \frac{e^{-sR/c}}{R} \qquad (2)$$

where

$$R = \left[(S_n - S'_n)^2 + a_n^2 \right]^{\frac{1}{2}} \qquad (3)$$

or

$$R = \left[S_n^2 + S'^2_m + a_n^2 \right]^{\frac{1}{2}} \qquad m \neq n \qquad (4)$$

To apply the SEM, (1) must be cast into matrix form and this may be accomplished by choosing as basis functions

$$I_{mk}(z) = \frac{\alpha_k \sin\left[-j\frac{s}{c}(z_{k+1} - z)\right] + \alpha_{k+1} \sin\left[-j\frac{s}{c}(z - z_k)\right]}{\sin\left[-j\frac{s}{c}(z_{k+1} - z_k)\right]} \tag{5}$$

where $z_k \leq z \leq z_{k+1}$ and z is the variable along any particular wire under consideration. The double subscript, mk, on I implies the current on the $m^{\underline{th}}$ wire in the $k^{\underline{th}}$ zone. Point matching is used and done in such a manner that for either geometry in Figure 1, the number of equations equals the number of unknowns. As shown by Otto and Richmond [6], the integrals in (1) reduce to algebraic expressions and (1) can be written as

$$\overline{\overline{\Pi(s)}}\ \overline{I(s)} = \overline{E(s)} \tag{6}$$

where the double line indicates a square matrix and the single line a column matrix.

The natural frequencies are defined as those values of s for which the left side of (6) becomes zero and for which a non-trivial solution for $\overline{I(s)}$ exists. Thus, at the natural frequencies, denoted by s_α the determinant of $\overline{\overline{\Pi(s)}}$ must be zero;

$$\overline{\overline{\Pi(s_\alpha)}}\ \overline{I(s_\alpha)} = 0 \tag{7}$$

$$\left|\overline{\overline{\Pi(s_\alpha)}}\right| = 0 \tag{8}$$

It is from (8) that the s_α's are determined. In (7), $\overline{\overline{I(s_\alpha)}}$ is defined as the mode vector and

$$\overline{\overline{\Pi(s_\alpha)}}^{\,T}\ \overline{\overline{C(s_\alpha)}} = 0 \qquad (9)$$

defines the coupling vector where $\overline{\overline{\Pi}}^{\,T}$ is the transpose of $\overline{\overline{\Pi}}$. Note that (7) and (9) determine $\overline{I}$ and $\overline{C}$ only to within multiplicative constants. Thus solutions to (7) and (9) will now be written as $C_{I_\alpha}\ \overline{\overline{I(s_\alpha)}}$ and $C_{C_\alpha}\ \overline{\overline{C(s_\alpha)}}$ where $\overline{I}$ and $\overline{C}$ are the "true" vectors. Baum [1] has shown that

$$\overline{\overline{i(t)}} = \sum_\alpha \overline{\overline{\overline{U(t)}}}\ \overline{\overline{I(s_\alpha)}}\ \overline{\overline{C(s_\alpha)}}^{\,T}\ \frac{\overline{E_o}}{s_\alpha}\, e^{s_\alpha t} \qquad (10)$$

for class 1 coupling coefficients with the normalization

$$\overline{\overline{C(s_\alpha)}}^{\,T}\ \left.\frac{\overline{\overline{d\Pi}}}{ds}\right|_{s=s_\alpha}\ \overline{\overline{I(s_\alpha)}} = 1 \qquad (11)$$

Note that (10) requires that no static response is possible. For the induced charge a static response term should be included (see the appendix). Thus in terms of solutions to (7) and (9), (10) is written as

$$\overline{\overline{i(t)}} = \sum_\alpha \frac{\overline{\overline{\overline{U(t)}}}\ C_{I_\alpha}\ C_{C_\alpha}\ \overline{\overline{I(s_\alpha)}}\ \overline{\overline{C(s_\alpha)}}^{\,T}\ \frac{\overline{E_o}}{s_\alpha}\, e^{s_\alpha t}}{C_{I_\alpha}\ C_{C_\alpha}}$$

and from (11)

$$C_{I_\alpha}\ C_{C_\alpha}\ \overline{\overline{C(s_\alpha)}}^{\,T}\ \left.\frac{\overline{\overline{d\Pi}}}{ds}\right|_{s=s_\alpha}\ \overline{\overline{I(s_\alpha)}} = C_{I_\alpha}\ C_{C_\alpha}$$

Therefore if the multiplicative constants are included in the solutions of the mode and coupling vectors,

$$\overline{\overline{i(t)}} = \sum_\alpha \frac{\overline{\overline{\overline{U(t)}}}\ \overline{\overline{I(s_\alpha)}}\ \overline{\overline{C(s_\alpha)}}^{\,T}\ \frac{\overline{E_o}}{s_\alpha}\, e^{s_\alpha t}}{C_{I_\alpha}\ C_{C_\alpha}}$$

and

$$\overline{C(s_\alpha)}^{T} \left.\frac{\overline{\overline{d\Pi}}}{ds}\right|_{s=s_\alpha} \overline{I(s_\alpha)} = C_{I_\alpha} C_{C_\alpha}$$

(10) becomes

$$\overline{i(t)} = \sum_\alpha \frac{\overline{\overline{U(t)}}\ \overline{I(s_\alpha)}\ \overline{C(s_\alpha)}^{T}\ \overline{\frac{E_o}{s_\alpha}}\ e^{s_\alpha t}}{\overline{C(s_\alpha)}^{T} \left.\frac{\overline{\overline{d\Pi}}}{ds}\right|_{s=s_\alpha} \overline{I(s_\alpha)}} \qquad (12)$$

$\overline{\overline{U(t)}}$ is a diagonal matrix with Heaviside functions along the main diagonal to take into account "turn-on" times and signal speeds, and $\overline{E_o}/s_\alpha$ is the excitation function for a step function that turns on at t = 0 and its singularity is included in an explicit fashion.

An expression analogous to (12) is derived in the appendix for computing the induced axial charge distribution.

3. NUMERICAL METHODS

A. Determination of Pole Locations

To determine the natural frequencies for a given geometry it is necessary to form $\overline{\overline{\Pi}}$ and solve (8) for the values of s_α. The particular numerical technique used in this work is Muller's method [7]. The advantages of this method are that multiple roots can be found, conjugate roots can be found, and no special formulation is needed to apply this to complex equations. In Muller's method the derivative of $\overline{\overline{\Pi}}$ is not used. While it is true that $\overline{\overline{d\Pi}}/ds$ is used in calculating the contribution of each sinusoid, it is calculated only once at the pole location and not several times as it would be in an iterative process. Approximate pole locations are not needed, though in practice having good estimates of pole locations will considerably reduce the number of iterations required to find the various roots.

In Muller's method, three approximations x_i, x_{i-1}, x_{i-2} are made to a root of the equation, $f(x) = 0$. The next approximation is found as a zero of the parabola which goes through the three points $(x_i, f(x_i))$, $(x_{i-1}, f(x_{i-1}))$, and $(x_{i-2}, f(x_{i-2}))$. Following Conte's development [7], define

$$f_i = f(x_i) \quad f_{i-1} = f(x_{i-1}) \quad f_{i-2} = f(x_{i-2})$$

and

$$f\left[x_i, x_{i-1}\right] = \frac{f_i - f_{i-1}}{x_i - x_{i-1}}$$

$$f\left[x_i, x_{i-1}, x_{i-2}\right] = \frac{f\left[x_i, x_{i-1}\right] - f\left[x_{i-1}, x_{i-2}\right]}{x_i - x_{i-2}}$$

The function $p(x)$

$$p(x) = f_i + f\left[x_i, x_{i-1}\right] (x - x_i)$$

$$+ f\left[x_i, x_{i-1}, x_{i-2}\right] (x - x_i)(x - x_{i-1})$$

is the unique parabola that passes through these three points. The roots of $p(x) = 0$ are determined from the quadratic formula. Writing $p(x)$ as

$$p(x) = a_o + a_1 x + a_2 x^2$$

The roots are

$$x = \frac{2\, a_o}{-a_1 \pm (a_1^2 - 4 a_o a_2)^{\frac{1}{2}}}$$

In Muller's method the sign is chosen such that the magnitude of the denominator is largest. This value of x is now taken as the approximation

x_{i+1} for the root. The process is repeated for x_{i+1}, x_i, x_{i-1}; etc. This is done until some criteria are met and the iteration stopped: e.g.

$$\left|x_{i+1}\right| - \left|x_i\right| < \varepsilon \tag{13}$$

and/or

$$\left|f(x_{i+1})\right| < \varepsilon \tag{14}$$

In the SEM, $\left|\overline{\overline{\Pi}}\right| = 0$ is the equation to be solved and any three starting values for s can be used. However, the closer to a root one starts the fewer iterations will be required. To find the second root of the determinant, the function is deflated or a new function is defined as

$$\left|\overline{\overline{\Pi}}\right| \Big/ (s - s_\alpha)\ (s - s_\alpha^*)$$

where s_α is the first root and, since in these SEM problems, s_α^* (complex conjugate = *) is also a root the term $s - s_\alpha^*$ is included. For real roots the $(s-s_\alpha^*)$ factor is omitted. As successive roots are found the function is similarly deflated. For a determinant formed from exponential functions as one has using sine functions as basis functions in this formulation, the number of roots to be found must be specified.

B. Calculation of Mode and Coupling Vectors

To calculate the mode vector associated with a particular s_α, $\overline{\overline{\Pi}}$ is evaluated at $s = s_\alpha$; the maximum pivot element is located and, if necessary, row and column interchanges are performed to move this element to the (1,1) position. By means of the Gauss-Jordan Reduction Technique with maximum pivot element the matrix is now upper triangularized. While it is true that

the root will likely never be found exactly by numerical means, it is true that by setting ε small (10^{-6}) in (13) [or (14)] the last diagonal element in the triangular matrix is usually five to seven orders of magnitude smaller than the other diagonal elements. This smallest element is set equal to zero, the last element of the mode vector is set equal to real one, and the remaining elements can now be calculated by the usual methods of linear algebraic equations. At this stage the mode vector components can be renormalized in any desired fashion. For example, Tesche [2] normalizes the mode vector such that the element having the largest magnitude is set equal to real one. In a like manner, the coupling vector is calculated from $\overline{\overline{\Pi}}(s_\alpha)^T$.

C. Coupling Coefficients for the Exponentially Damped Sinusoids

Baum [1,8] has outlined the means by which one can determine the contribution due to each damped sinusoid. In section 2 of this report these procedures are outlined, and (12) is the final result of the manipulations. Actually i(t) has been determined by two methods - that outlined in section 2 of this report and also by means of a limiting process such as equation (3.41) in [1]. Excellent agreement is found between the two methods.

4. Numerical Results

As a means of establishing the accuracy of the results obtained from the SEM, a study was made to determine the effects of zoning, types of current

expansions used, and the integral equation formulation employed on the values of the currents that are calculated at the center of the antenna in the frequency domain. The following summarizes these computations. All results are for a simple dipole (diameter/total length = d/L) excited by a monochromatic plane wave, incident broad-side, having a value such that $kL = 2\pi$. The first capital letter in the heading refers to Pocklington (P) or Hallen (H) theory and the second to the basis functions (current expansions) used - piecewise sinusoids (S), piecewise constant (C). All currents are ma/volt.

No. of Zones	Real I	Imag. I
	P - S, d/L = 0.1	
20	10.404	-12.812
40	10.228	-13.398
90	09.968	-14.026
	P - C, d/L = 0.1	
20	10.574	-12.708
40	10.276	-13.362
90	9.963	-13.987
	H - C, d/L = 0.1	
20	10.455	-13.056
40	10.221	-13.489
90	9.925	-14.087
	P - S, d/L = 0.013	
20	1.745	-6.140
40	2.823	-7.710
90	3.314	-8.332

	P - C, d/L = 0.013	
20	3.421	-8.295
40	3.517	-8.204
90	3.405	-8.316
	H - C, d/L = 0.013	
20	3.386	-8.359
40	3.369	-8.374
90	3.358	-8.389

Thus for thick wires (d/L = 0.1) the various results agree to within a few percent for any number of zones. However for thin wires (d/L = 0.013) P - S gives results that are low by about 30% when 20 zones are used. Since the running time is proportional to the square of the number of zones, these results suggest that P - S should not be used for thin structures. The advantage of P - S is that the matrix elements are algebraic expressions and involve no numerical integrations. This advantage is outweighed for thin wires by the fact that a large number of zones must be used to obtain accurate results.

In Figure 2 the pole locations for a cylinder with d/L = 0.01 are shown as determined by Tesche [2] and this approach. Notice that the pole locations are sensitive to zoning in the same manner as the currents in the frequency domain. Figure 3 shows the effects of zoning on pole locations for a cylinder with d/L = 0.1. In Figures 4 and 5 are plots of the mode vectors for two different cylinders, two poles on each cylinder and different zoning. For the thin cylinder, the mode vector changes very little as the zoning increases from 18 zones/meter to 40 zones/meter. For the thick cylinder, the mode vector shows oscillations near the ends of the cylinder

at 40 zones/meter. This is due to the thin-wire approximation and the fact that no end corrections are included.

Figure 6 is the time history of the current on a thin dipole for broadside incidence. This is determined from the two poles having the smallest magnitude (Figure 2). However, the second pole makes no contribution to the current at any point along the cylinder. This agrees with Sassman's results [3] which show strong resonances at $kL/2 = 1.2$ and the next at $kL/2 = 4$. In view of these results, Figure 7 is $i(t)$ for the thick cylinder for the smallest (first) pole and then, at early time, $i(t)$ is shown for the first and third poles (Figure 3) at two locations along the antenna. The agreement between these results and those previously obtained [3,4] is quite good. For ct/L greater than 4, the contribution of the third pole is negligible at either position.

Figure 8 shows various poles calculated for the crossed cylinder model assuming excitation along the y-axis. In this particular geometry equal length cylinders are considered and $d/L = 0.1$ for each. Also, in the interest of running time, the problem is zoned at 12 zones/meter. Figures 9, 10 and 11 are current time histories for this problem with different numbers of poles used and at the junction on the different wires in the problem. It appears that for $ct/L > 3$, two poles provide good results while for $ct/L < 3$, additional ones must be considered. The curves are calculated using the same excitation and are to be compared to Figures 23, 24 and 25 in reference 4. (In the two reports, the curves for the x-axis have different signs since they were plotted for different sides of the junction.)

Literature Cited

1. Baum, C. E., "On the Singularity Expansion Method for the Solution of Electromagnetic Interaction Problems," EMP Interaction Note 88, Dec. 1971.

2. Tesche, F. M., "On the Singularity Expansion Method as Applied to Electromagnetic Scattering from Thin-Wires," EMP Interaction Note 102, Apr. 1972.

3. Sassman, R. W., "The Current Induced on a Finite, Perfectly Conducting, Solid Cylinder in Free Space by an Electromagnetic Pulse," EMP Interaction Note 11, Jul. 1967.

4. Taylor, C. D. and Crow, T. T., "Induced Electric Currents on Some Configurations of Wires, Part I, Perpendicular Crossed Wires," EMP Interaction Note 85, Nov. 1971.

5. Mei, K. K., "On the Integral Equations of Thin Wire Antennas," IEEE Trans. Ant. Prop., Vol. AP-13, No. 3, 1965, pp 374-378.

6. Otto, D. V. and Richmond, J. H., "Rigorous Field Expressions for Piecewise-Sinusoidal Line Sources," IEEE Trans. Ant. Prop., Vol. AP-17, no. 1, 1969, p. 98.

7. Conte, S. D. and de Boor, C., ELEMENTARY NUMERICAL ANALYSIS, McGraw-Hill Book Co., New York (1972).

8. Baum, C. E., "On the Singularity Expansion Method for the Case of First Order Poles," EMP Interaction Note 129, Oct. 1972.

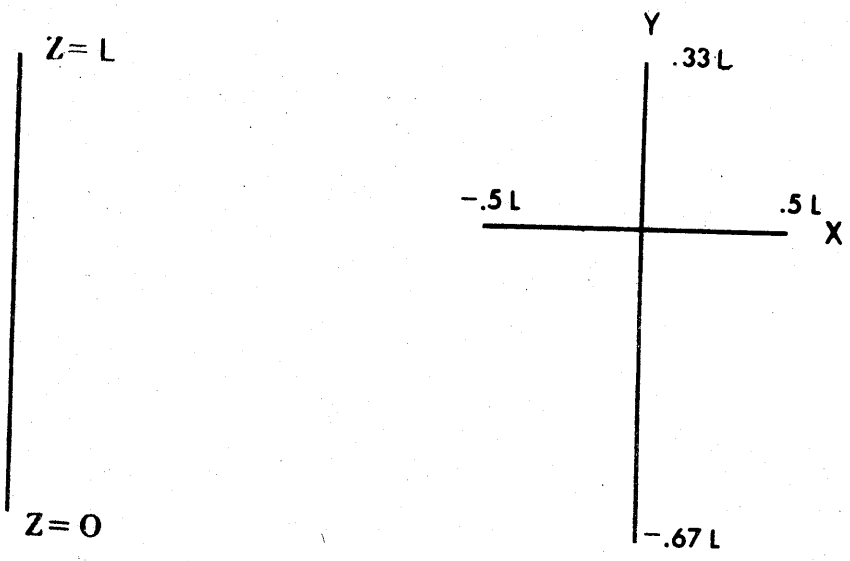

Fig. 1. The geometries of the scatterers considered.

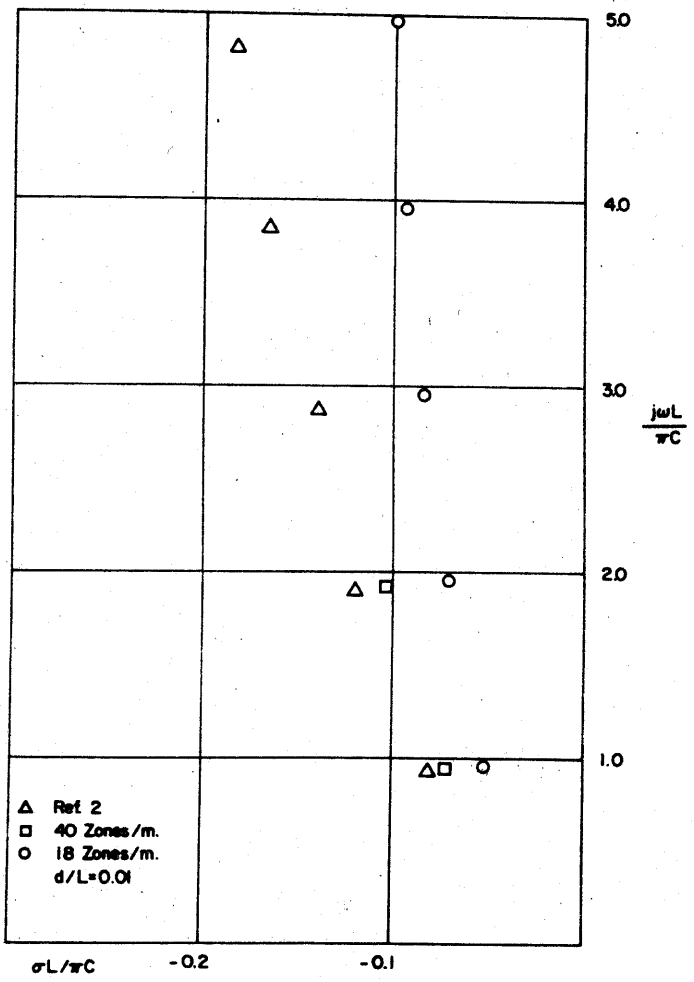

Fig. 2. Pole locations for a cylinder with d/L = 0.01.

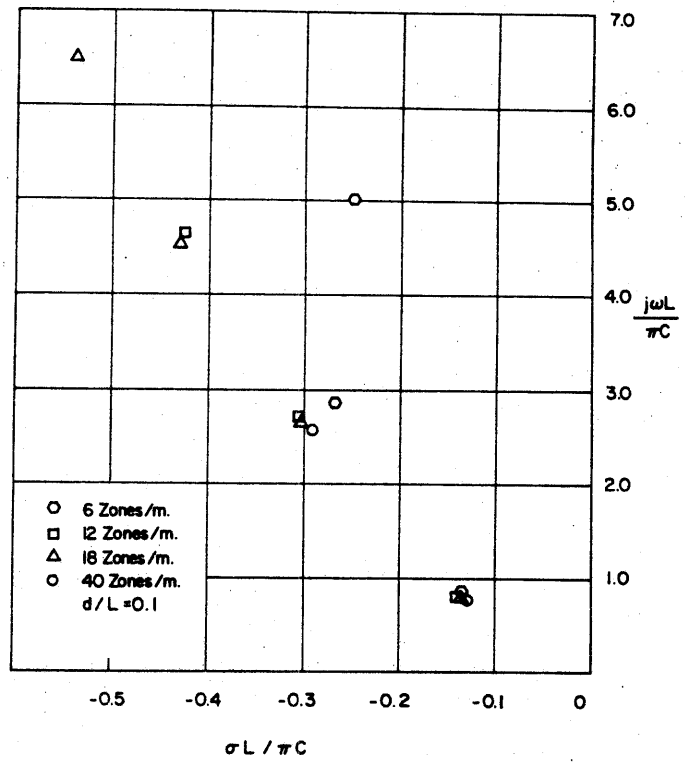

Fig. 3. Pole locations for a cylinder with d/L = 0.1.

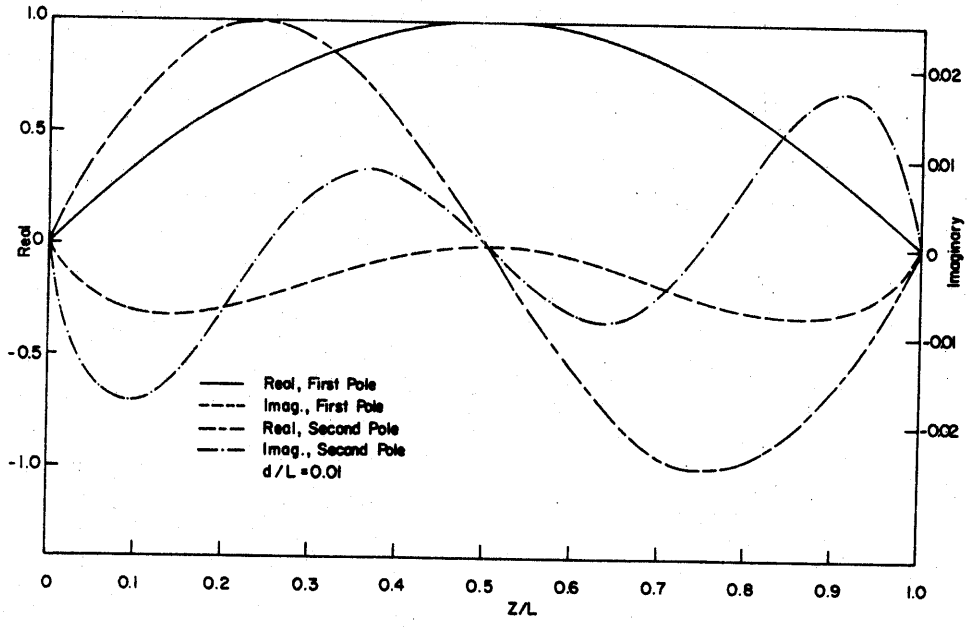

Fig. 4. Normalized mode vectors for a cylinder with d/L = 0.01.

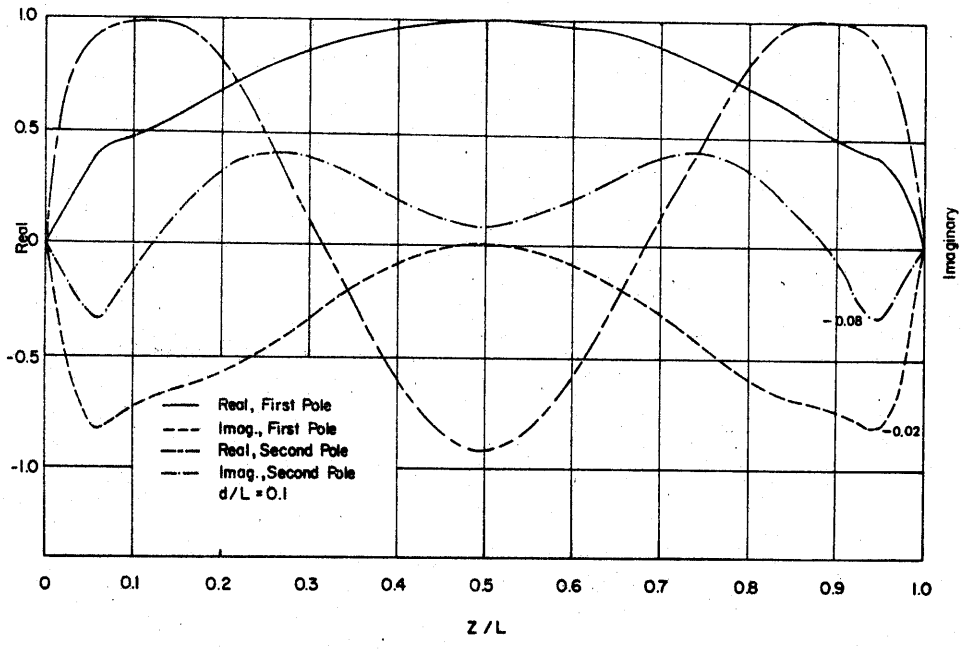

Fig. 5. Normalized mode vectors for a cylinder with d/L = 0.1.

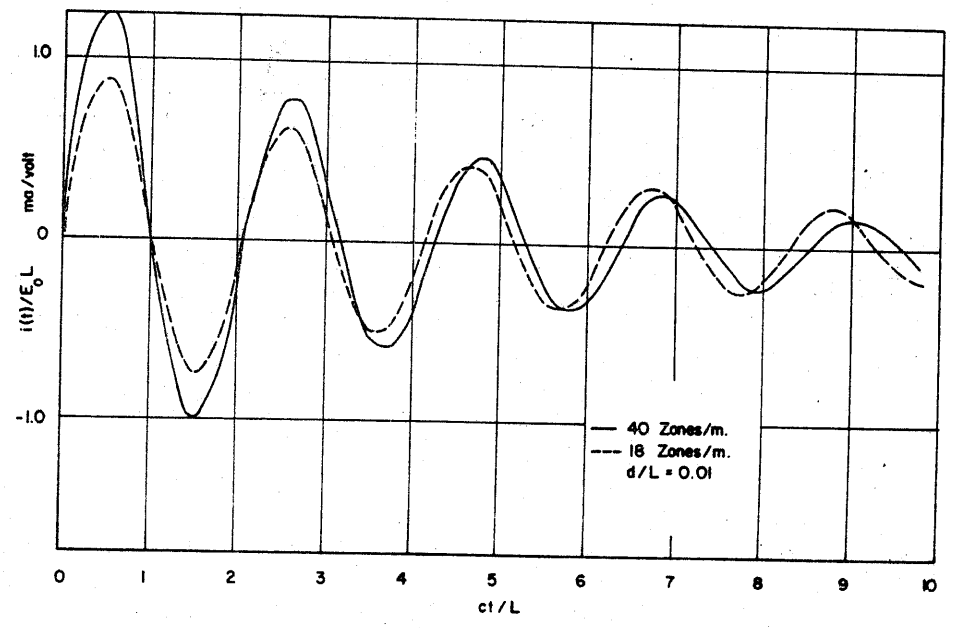

Fig. 6. Current on a cylinder with d/L = 0.01.

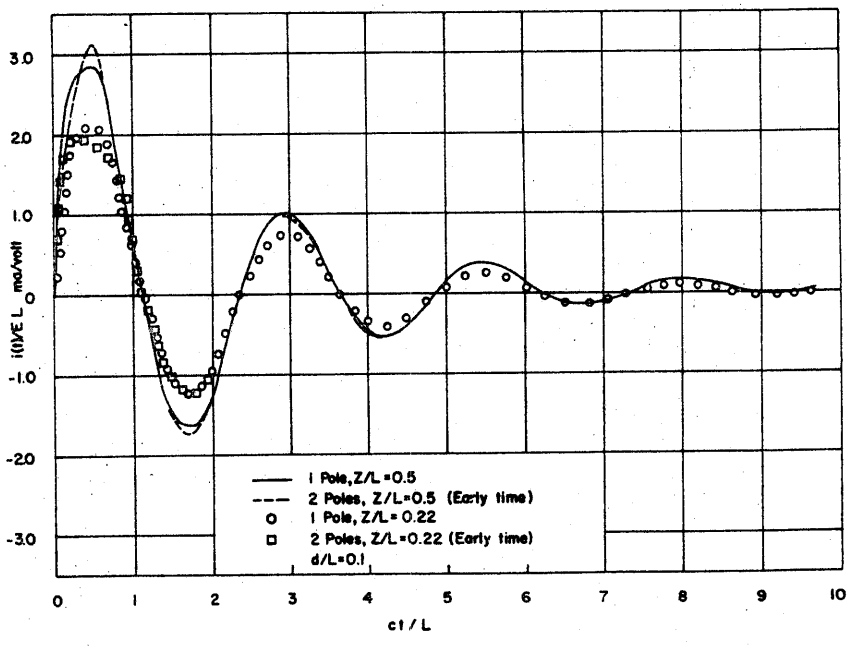

Fig. 7. Current on a cylinder with d/L = 0.1.

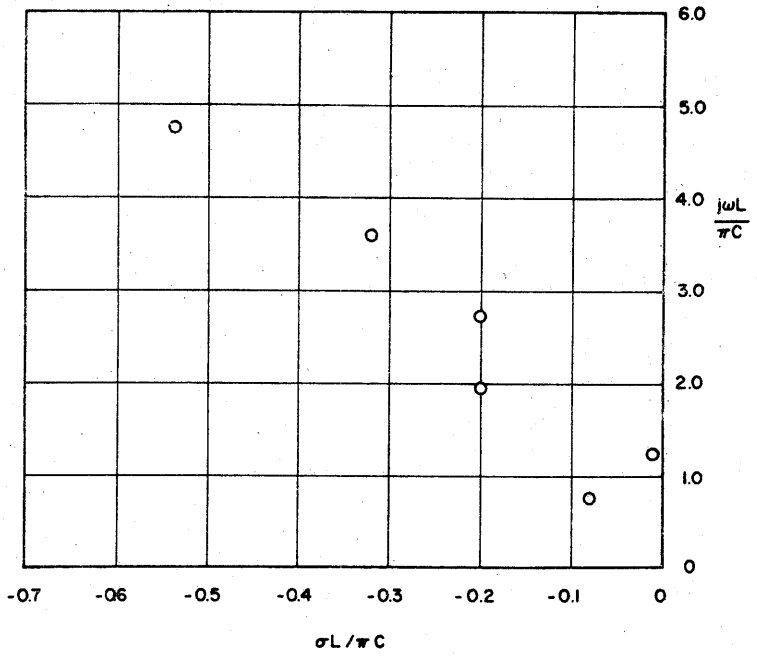

Fig. 8. Pole locations for the crossed cylinder geometry.

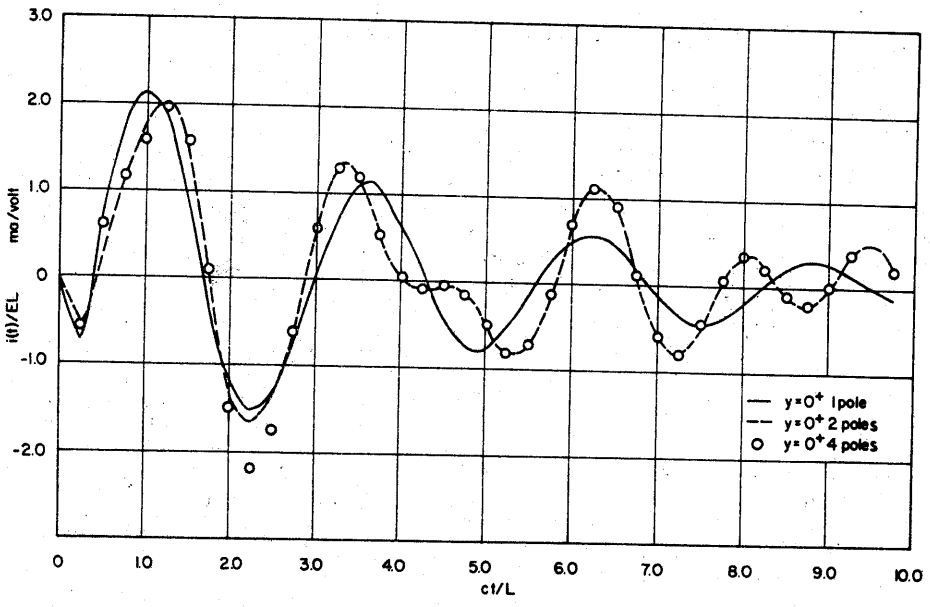

Fig. 9. Current near the junction in the crossed cylinder geometry.

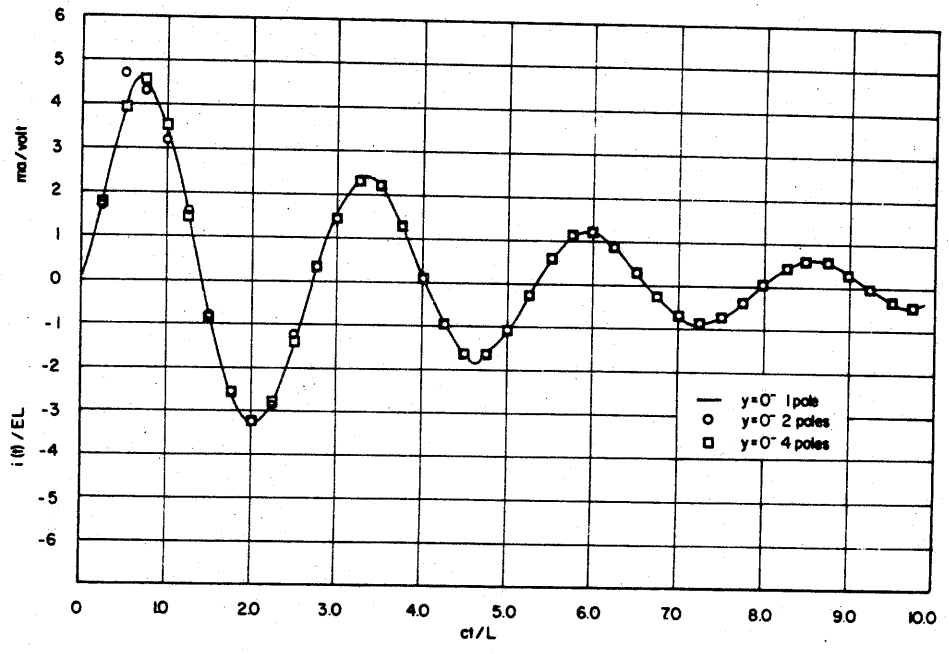

Fig. 10. Current near the junction in the crossed cylinder geometry.

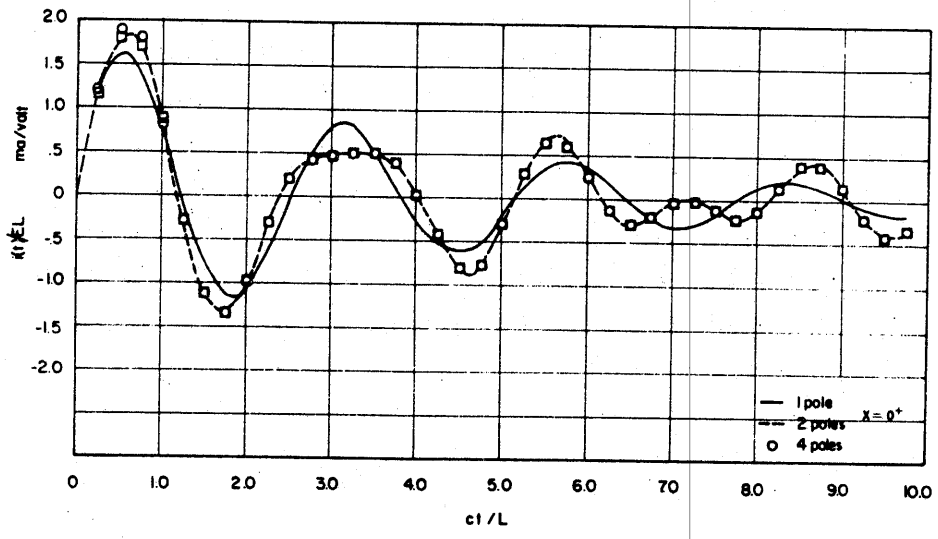

Fig. 11. Current near the junction in the crossed cylinder geometry.

APPENDIX

In addition to providing a means by which the current time histories may be evaluated, the SEM provides a convenient means by which charge densities may be obtained. In section 2 of this report the method for calculating i(t) has been outlined. Baum [1] and Tesche [2] have discussed the necessary operations using the continuity equation to obtain the charge density. This expression is

$$\overline{\rho(t)} = -\frac{1}{2\pi j}\int \sum_{\alpha} \overline{\overline{U(t)}}\ \overline{D(s_\alpha)}\ \overline{C(s_\alpha)}^{T}\ \frac{\overline{E_o(s)e^{st}}}{s^2(s-s_\alpha)}\,ds$$

where

$$\overline{D(s_\alpha)} = \frac{d}{dz}\,\overline{I(s_\alpha)}$$

Taking into account the second order pole one obtains

$$\begin{aligned}\overline{\rho(t)} = &-\sum_{\alpha} \overline{\overline{U(t)}}\ \overline{D(s_\alpha)}\ \overline{C(s_\alpha)}^{T}\ \frac{\overline{E_o(s_\alpha)}}{s_\alpha^2}\ e^{s_\alpha t}\\ &+\sum_{\alpha} \overline{\overline{U(t)}}\ \overline{D(s_\alpha)}\ \overline{C(s_\alpha)}^{T}\ \frac{\overline{E_o(0)}}{s_\alpha^2}\\ &+ t\sum_{\alpha} \overline{\overline{U(t)}}\ \overline{D(s_\alpha)}\ \overline{C(s_\alpha)}^{T}\ \frac{\overline{E_o(0)}}{s_\alpha}\\ &+\sum_{\alpha} \overline{\overline{U(t)}}\ \overline{D(s_\alpha)}\ \overline{C(s_\alpha)}^{T}\ \frac{\overline{E_o'(0)}}{s_\alpha}\end{aligned} \qquad \text{(1a)}$$

Notice that in (1a) the particular form of the excitation function, namely a step function that turns on at t = 0, has been used and the form of (1a) depends on the inclusion of the explicit 1/s dependence of this function. Since the coefficient of t in (1a) must be zero, it follows that

$$\left\{ \sum_{\alpha} \overline{\overline{U(t)}}\ \overline{D(s_\alpha)}\ \overline{\frac{C(s_\alpha)}{s_\alpha}}^{T} \right\} \overline{E_o(0)} = 0 \qquad (2a)$$

This is true irrespective of the form of E_o; thus

$$\sum_{\alpha} \overline{\overline{U(t)}}\ \overline{D(s_\alpha)}\ \overline{\frac{C(s_\alpha)}{s_\alpha}}^{T} = \overline{0}^{T} \qquad (3a)$$

where $\overline{0}^{T}$ is the transpose of the null column vector.

The last term in (1a) involves the sum (3a) and thus makes a zero contribution to the charge density. Therefore,

$$\rho(t) = -\sum_{\alpha} \overline{\overline{U(t)}}\ \overline{D(s_\alpha)}\ \overline{C(s_\alpha)}^{T}\ \overline{\frac{E_o(s_\alpha)}{s_\alpha^2}}\ e^{s_\alpha t}$$

$$+\sum_{\alpha} \overline{\overline{U(t)}}\ \overline{D(s_\alpha)}\ \overline{C(s_\alpha)}^{T}\ \overline{\frac{E_o(0)}{s_\alpha^2}} \qquad (4a)$$

and all terms are defined.